Application of the DEM in Simulation of the Media Motion in a Wet Bead Mill

Application of the DEM in Simulation of the Media Motion in a Wet Bead Mill

By DARIUSZ GUDIN*1, JUNYA KANO*1and FUMIO SAITO*1

The DEM (Discrete Element Method) technique for simulating the grinding media motion in a wet bead mill has been developed. Additional parameters related to the flow of slurry inside a grinding chamber have been introduced to the standard DEM code. The grinding beads motion was simulated and compared with real motion recorded with a video camera. From the beads motion the specific impact energy of the beads was calculated and compared with the grinding rate constant of a gibbsite powder sample obtained experimentally. It was shown that the correlation between experimental and simulated data makes it possible to predict the grinding performance of the mill for given conditions at the base of the computer simulation.

(Received Decembar 13, 2006)

Keywords: *wet grinding, discrete element method, beads motion, impact energy*

1 Introduction

Due to rapidly growing interest in application of ultra fine particles in science and industry, fine grinding has been paid much attention in the field of nano-technology. Fine grinding is to reduce the particle size into 100 μm or so, although recently there has been increasing requirement for finer size of particles down to submicron to nano-meter orders. To satisfy this demand many types of new mills have been developed. One of them is a wet bead mill, which is capable of effectively producing sub-micron particles, due to attrition brakeage mechanism employed to reduce the particle size of a powder material. Basically the wet bead mill consists of a grinding chamber with an agitator, armed with a set of disc or pins, and a slurry tank connected with a circulation system. The chamber is filled with grinding beads and a slurry, and the beads motion depends on the revolutions of the agitator, driven by an electric motor. Powder particles are ground by the colliding motion of the beads and hence the grinding effect is dependent on the beads behaviour, which can be controlled by many operating parameters such as the rotational speed of the agitator, the beads filling ratio, their diameter and material, the slurry concentration, and the like. Therefore, a certain number of research works on influence of operating conditions on the bead motion and grinding performance has been reported [1–7].

Meanwhile, the Discrete Element Method (DEM), proposed by Cundall and Strack [8], makes it possible to trace precisely the motion of each grinding bead and calculate its velocity and acceleration as well as forces acting on it. The DEM is one of the most popular techniques for simulating and analyzing the solid particle behaviour and has been successfully applied in many fields such as soil and rock mechanics, agricultural product handling, storage and flow of granular materials, particle motion in fluidized beds, and so on. Since Mishra and Rajamani [9] adopted in 1992 the DEM technique to solve tumbling mill problems, a significant number of researches on the simulation of grinding in different types of mills have been reported [10–13]. However, the original DEM technique has been developed for dry systems and hence, in order to apply it to simulation of the wet bead milling operation, adequate modifications have to be introduced.

This work describes our research into adoption of the DEM technique to simulation of the

*1 Institute of Multidisciplinary Research for Advanced Materials, Tohoku University, Sendai, 80-8577, Japan

beads motion under wet conditions, and applicability of the proposed method to prediction of the grinding performance of the wet bead mill, on the basis of the computer simulation.

2 Simulation

The fundamental assumption of the DEM is that the simulated material consists of discrete bodies, which may have different shapes and properties and can interact with their nearest neighbors. Therefore, the method is perfectly fit for simulating the behaviour of non-continuous materials. In the simulation, the shapes of the grinding chamber and the agitator are constructed with a series of planes, and the agitator is a full cylinder with nine pins, without openings. The contact on collision between two bodies is expressed by the simulation model shown in Fig.1, which consists of a spring, a dashpot and a slider. The interactive force $\boldsymbol{F}_i$ at the collision is calculated from Eq.(1), where K and η are the spring and damping coefficients respectively and $\boldsymbol{u}$ is the relative displacement.

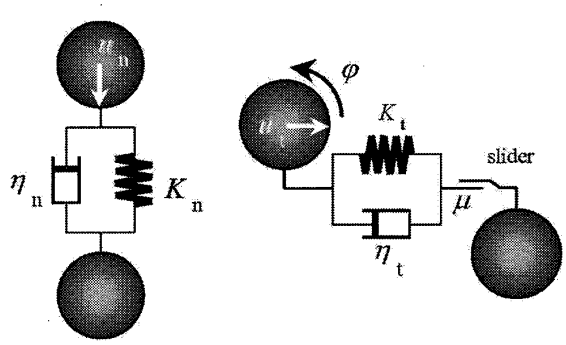

Fig.1 Model of interactive forces between two media beads [10].

$$\boldsymbol{F}_i = K\boldsymbol{u} + \eta\frac{d\boldsymbol{u}}{dt} \tag{1}$$

The motion of a bead is calculated from the Newton's Second Law described by Eq.(2), where a denotes the acceleration of the bead, m is the mass of the bead, g is the gravitational acceleration and F is the total resultant force.

$$\boldsymbol{a} = \frac{\boldsymbol{F}}{m} + \boldsymbol{g} \tag{2}$$

The motion of beads under wet condition is influenced by a powder sample suspension, therefore additional parameters, related to the presence and the flow of slurry, have to be taken into account. The drag force F_D is calculated by Eq.(3), where C_d is the drag coefficient, A is the projection area of the bead, ρ_s is the density of slurry and u_r is the relative velocity between the bead and slurry.

$$\boldsymbol{F}_D = C_d A \rho_s \frac{\boldsymbol{u}_r^2}{2} \tag{3}$$

The C_d is calculated by Eq.(4) [14] and Eq.(5), where d_B denotes the bead diameter and α is the viscosity of slurry.

$$C_d = \frac{23.5}{\mathrm{Re}} + \frac{4.6}{\sqrt{\mathrm{Re}}} + 0.3 \tag{4}$$

$$\mathrm{Re} = \frac{d_B \mid \boldsymbol{u}_r \mid \rho_s}{\alpha} \tag{5}$$

The circular flow rate of the slurry is modeled by Eq.(6) [15], where r is the radius and v_θ is the slurry velocity. Close to the lids of the chamber a linear reduction of the slurry velocity is introduced.

$$\frac{d}{dr}\left[\frac{1}{r}\frac{d}{dr}(r\boldsymbol{v}_\theta)\right] = 0 \tag{6}$$

The buoyant force F_B for beads is calculated by Eq.(7), where V_B is the volume of the bead.

$$\boldsymbol{F}_B = V_B \rho_s \tag{7}$$

The friction coefficient is one of the most important parameters in the DEM simulation. Its value can be estimated by comparing the motion simulated with that observed in experiments. Unlike in dry grinding, in wet conditions powder particles do not cover fully surfaces of grinding media and direct contact between colliding bodies can exist. Therefore separated values of the friction coefficient for bead-bead and bead-wall interactions are determined. In researched conditions the values of the friction coefficients between beads and between a bead and the wall are $\mu_i = 0.2$ and $\mu_w = 0.25$ respectively. Parameters used in the calculation are shown in Table 1.

Table1 Constants used in the calculation.

Beads density[g/cm^3]	6.0
Young's modulus[GPa]	21.0
Poisson's ratio[−]	0.30
Time step[s]	1.1×10^{-6}
Slurry density[kg/m^3]	1029
Slurry dynamic viscosity[mPa · s]	1.1

3 Experimental

The mill used in the experiment is a bead mill (MiniZeta, NETZSCH, Germany). The schematic diagram of the experimental equipment is shown in Fig.2. The horizontally positioned grinding chamber and the agitator are made of stainless steel. In order to visualize the beads motion, the original grinding chamber was replaced with transparent one. The dimensions of the chamber

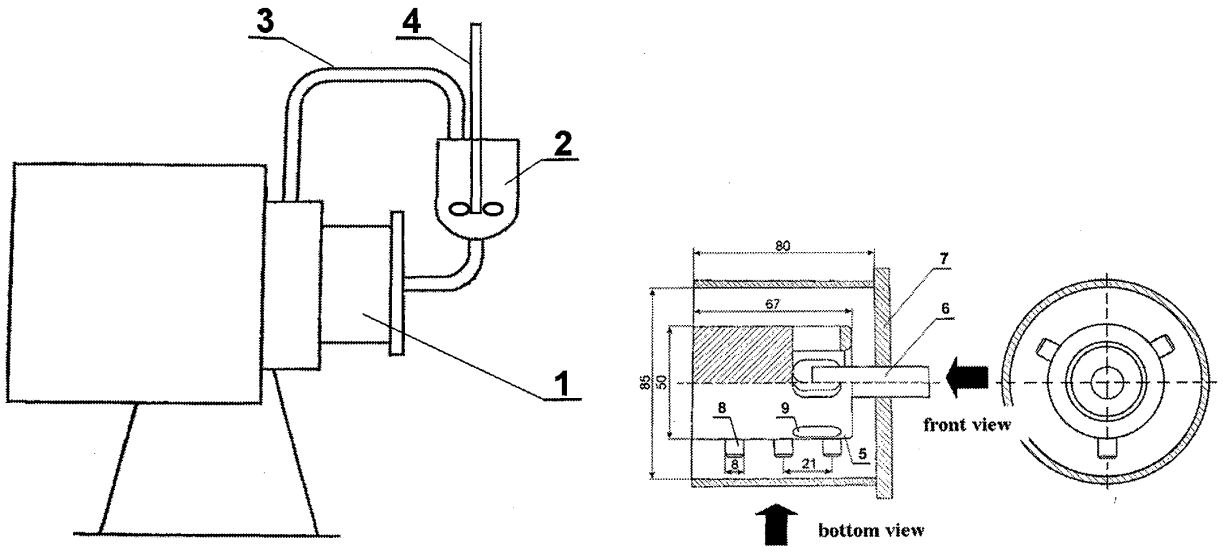

(a)-mill: 1-grinding chamber, 2-slurry tank, 3-recirculation system, 4-mixer

(b)-grinding chamber: 5-agitator, 6-connector pipe, 7-front lid, 8-pin, 9-opening

Fig.2 Schematic diagram of the bead mill.

are 85 mm diameter and 80 mm length. Free volume of the chamber is 350 cm^3. Between the front lid and the agitator there is a gap 13 mm wide. The agitator is a partly hollow cylinder 50 mm in diameter, with six elongated openings and nine cylindrical pins, as shown in Fig.2b. Three sets of yttrium stabilized zirconia beads (YSZ) 1.5, 2.0 and 3.0 mm in diameter were used. The volume of each set of the beads was 200 cm^3. The movement of the beads near transparent parts of the chamber was observed from the front and the bottom view at 600, 800, 1000, 1200, 1800 and 2400 rpm in rotational speed of the agitator and recorded with a digital video camera. A sample used in the experimental work was gibbsite ($Al(OH)_3$, Sumitomo Chemical Co., Ltd, Japan). The 10%, 50% and 90% initial particle size were 39.55, 56.8, 83.79 μm, respectively. The initial particle size and the reduction in the particle size during grinding were determined by using a particle size analyzer (Microtrac S3000, Nikkiso, Japan). The sample was dispersed in water at the solid concentration 5.0 wt.%. Conditions of the experiments are shown in Table 2.

Table2 Experimental conditions.

Grinding chamber vol.[cm^3]	350					
Rotational speed[rpm]	600	800	1000	1200	1800	2400
Beads volume[cm^3]	200					
Beads diameter[mm]	1.5		2.0		3.0	
Slurryconcentration[%]	5.0					

4 Results and Discussion

4.1 Beads motion in the mill

In order to confirm applicability of the proposed method to the simulation of the beads motion in the bead mill under wet conditions, the simulated results were compared with the real movement of the grinding media, recorded by the video camera. Measurement and comparison of the velocity of the beads at the line marked in Fig.3 helps us to asses the results. Fig.4 presents the experimental and calculated velocities of the beads at the agitator speeds of 600 and 1200 rpm. Due to difficulty with observation of the beads motion close to the centre of the front lid, this space is not evaluated. According to expectations, the velocity of the beads increases with an increase in the rotational speed of the agitator. Close to the lids the

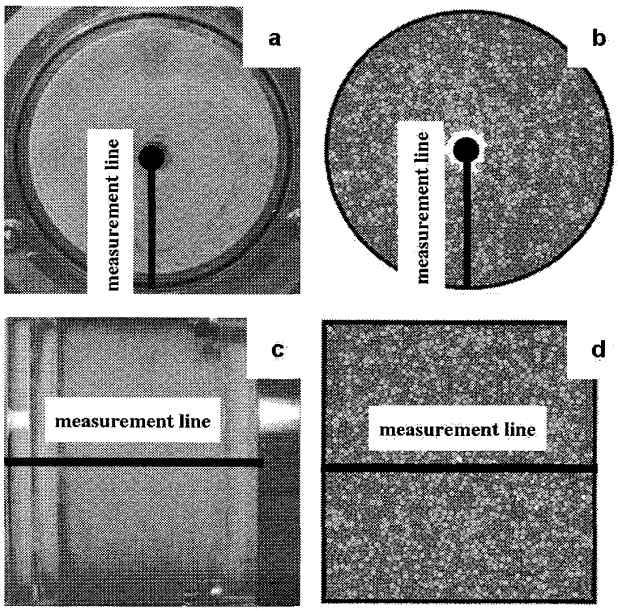

Fig.3 Beads motion in wet condition (d_B=2 mm, N=1200 rpm). a and c –real motion, b and d – simulation

beads motion is slower than that inside the chamber. This may be a result of the friction of the beads against the lids. The simulated data are satisfactorily consistent with experimental ones.

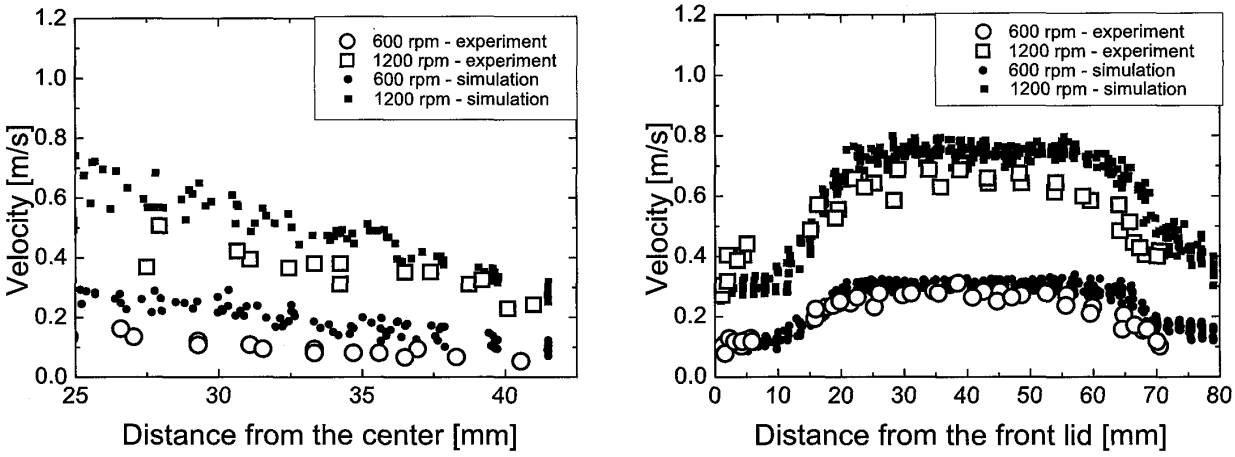

(a)–front view (b)–bottom view

Fig.4 Velocity of the beads in wet conditions(d_B=2 mm).

4.2 Calculation of the grinding rate constant and the specific impact energy

Figs.5 and 6 show the normalized 50% particles size $(D_t - D_l)/(D_0 - D_l)$ as a function of the grinding time t, for various values in the rotational speed of the agitator and the diameter of the beads, respectively. The plotted values are experimental data and the lines are calculated from Eq.(8), where K_P denotes the grinding rate constant, D_t is the 50% particle size at arbitrary grinding time, D_l is the 50% particle size of the finest sample among all experiments and D_0 is the 50% particle size at initial stage.

$$\frac{D_t - D_l}{D_0 - D_l} = exp\left(-K_p t^{0.25}\right) \tag{8}$$

As can be seen, extension of the grinding time causes a decrease in the particle size, although the

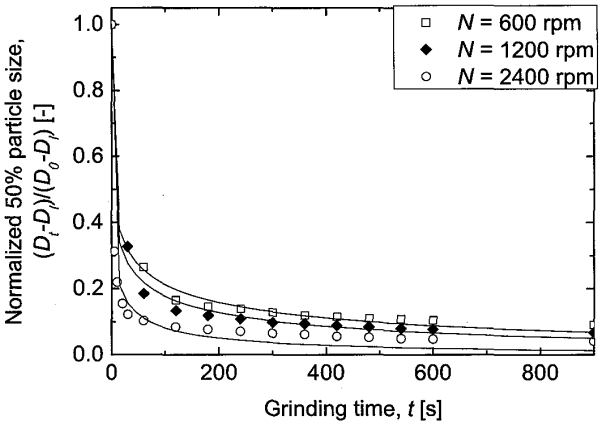

Fig.5 Normalized 50% particle size for various values of the rotational speed of the agitator N (d_B=2 mm).

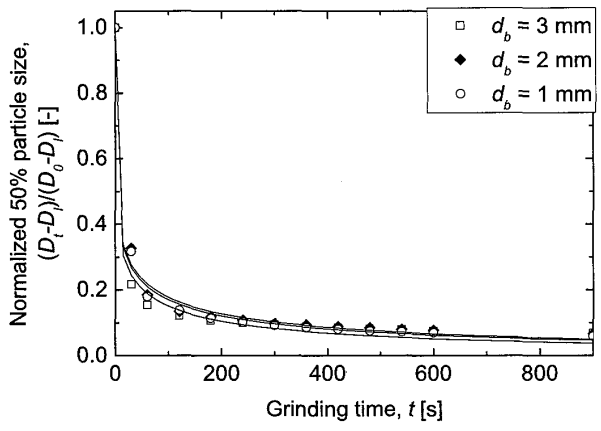

Fig.6 Normalized 50% particle size for different bead diameters (N=1200 rpm).

quickest size reduction occurs at the beginning of the operation. Increasing the rotational speed improves the grinding performance. Influence of the diameter of the beads on grinding effect is much less significant.

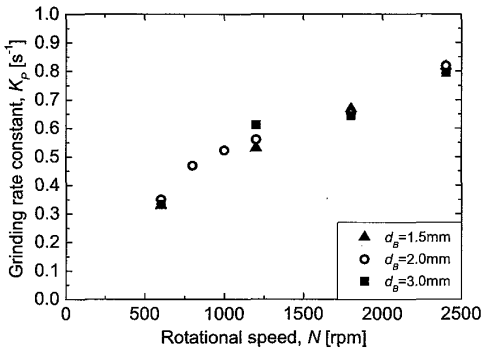

Fig.7 Grinding rate constant as a function of the rotational speed of the agitator.

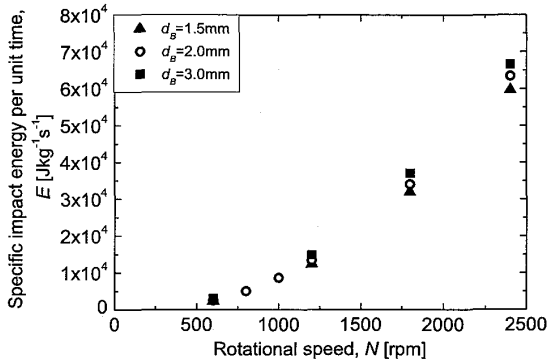

Fig.8 Specific impact energy per unit time as a function of the rotational speed of the agitator.

Fig.7 shows the grinding rate constant, defined by Eq.8, as a function of the rotational speed for three sets of beads. The grinding rate constant increases linearly with an increase in the rotational speed, however below 1200 rpm its value decreases dramatically. Distinct effect of the diameter of the beads is not affirmed.

Fig.8 illustrates the specific impact energy per unit time E_W, calculated by Eq.9, as a function of the rotational speed for all sets of the beads. In the equation W denotes the mass of the sample charged in the mill and t_s is the simulation time. Similar trend to that between grinding rate constant and rotational speed is shown. An increase in the rotational speed causes high specific impact energy, and clear influence of the diameter of the beads is not observed.

$$E_w = \frac{\sum \frac{1}{2} m v_j^2}{W \cdot t_s} \tag{9}$$

4.3 Prediction of the size reduction of a sample

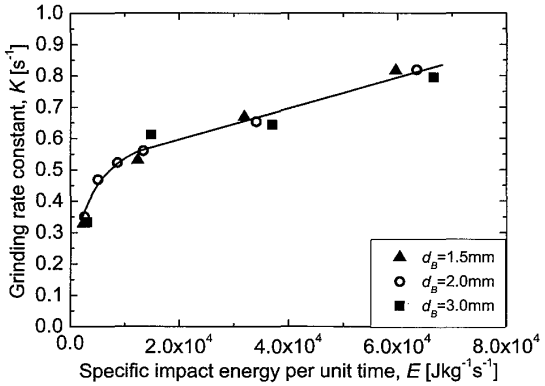

Fig.9 Relation between the specific impact energy and the grinding rate constant.

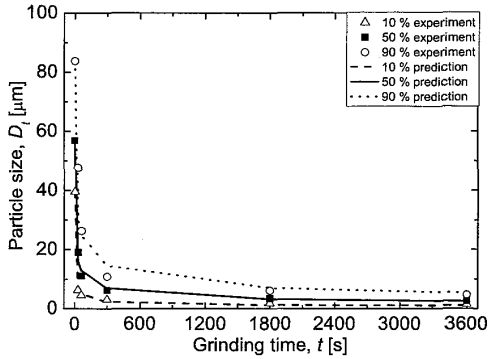

Fig.10 Predicted particle size of the sample ground for various periods of time (d_B=2 mm, N=1200 rpm).

Fig.9 presents the relationship between the grinding rate constant and the specific impact energy for all conditions. The correlation between them confirms that the specific impact energy calculated by the proposed method would be useful for predicting the grinding rate constant and the particle size reduction.

Fig.10 shows relation between the particle size and time of grinding for 10%, 50% and 90% particle size. The plotted points are experimental data and the lines represent predicted values. The experimental results are well consistent with predicted ones.

5 Conclusions

The modified DEM technique for simulating the grinding media motion under wet conditions, and applicability of the proposed method to prediction of the grinding performance of the wet bead mill has been presented in this work. In order to reflect the wet environment inside the grinding chamber, additional parameters related to presence and flow of slurry have been introduced to the standard DEM simulation code. The specific impact energy calculated at the base of the grinding media motion simulated was compared with the grinding rate constant of the gibbsite powder determined experimentally. The following conclusions can be formulated:

1. The velocity of the beads simulated by the modified DEM technique is consistent with that measured experimentally. It confirms applicability of the proposed method for simulating the particle motion in wet conditions.
2. The experimental and simulated velocity of the beads as well as the grinding rate constant and the specific impact energy increase with an increase in the rotational speed of the agitator. Distinct influence of the diameter of the beads on the grinding performance of the mill has not been affirmed.
3. Correlation between the grinding rate constant and the specific impact energy makes possible to predict the size reduction of a sample on the basis of the computer simulation.

Nomenclature

A projection area of grinding media [m^2]
a acceleration [$m \cdot s^{-2}$]
C_d drag coefficient [-]
D_0 50% particle size at initial stage [μm]
D_l 50% particle size of the finest sample among all experiments [μm]
D_t 50% particle size at arbitrary grinding time [μm]
d_B bead diameter [m]
E_w specific impact energy of beads per unit time [$J \cdot kg^{-1} \cdot s^{-1}$]
F resultant force [N]
F_B buoyant force [N]
F_D drag force [N]
F_i interactive force [N]
g gravitational acceleration [$m \cdot s^{-2}$]
K spring coefficient [-]

K_P grinding rate constant [s^{-1}]
m mass of grinding media [kg]
N rotational speed of the agitator [rpm]
r radius [m]
Re Reynolds number [-]
t grinding time [s]
t_s simulation time [s]
u displacement [m]
u_r relative velocity between the bead and suspension [$m \cdot s^{-1}$]
V_B volume of the bead [m^3]
v_j relative velocity of beads on collision [$m \cdot s^{-1}$]
v_θ slurry velocity [$m \cdot s^{-1}$]
W mass of sample [kg]
α viscosity of slurry [mPa·s]
η damping coefficient [-]
μ_i coefficient of friction between beads [-]
μ_w coefficient of friction between a bead and the wall [-]
ρ_s density of suspension [$kg \cdot m^{-3}$]

文 献

[1] Belaroui K., Pons M. N., Vivier H., and Meijer M. Wet grinding of gibbsite in a bead-mill. *Powder Technology*, Vol. 105, No. 1-3, pp. 396–405, 11 1999.

[2] Becker M., Kwade A., and Schwedes J. Stress intensity in stirred media mills and its effect on specific energy requirement. *International Journal of Mineral Processing*, Vol. 61, No. 3, pp. 189–208, 3 2001.

[3] Bel Fadhel H. and Frances C. Wet batch grinding of alumina hydrate in a stirred bead mill. *Powder Technology*, Vol. 119, No. 2-3, pp. 257–268, 9 2001.

[4] Blecher L. and Schwedes J. Energy distribution and particle trajectories in a grinding chamber of a stirred ball mill. *International Journal of Mineral Processing, Comminution*, Vol. 44-45, pp. 617–627, 3 1996.

[5] Blecher L., Kwade A., and Schwedes J. Motion and stress intensity of grinding beads in a stirred media mill. part 1: Energy density distribution and motion of single grinding beads. *Powder Technology*, Vol. 86, No. 1, pp. 59–68, 1996.

[6] Theuerkauf J. and Schwedes J. Theoretical and experimental investigation on particle and fluid motion in stirred media mills. *Powder Technology*, Vol. 105, No. 1-3, pp. 406–412, 1999.

[7] Eskin D., Zhupanska O., Hamey R., Moudgil B., and Scarlett B. Microhydrodynamics of stirred media milling. *Powder Technology, Particle Technology Forum Special Issue - Papers presented in the Particle Technology Forum sessions at the 2003 Annual AIChE meeting in San Francisco*, Vol. 156, No. 2-3, pp. 95–102, 2005.

[8] Cundall P. A. and Strack O. D. L. A discrete numerical model for granual assemblies. *Geotechnique*, Vol. 29, pp. 47–65, 1979.

[9] Mishra B. K. and Rajamani R. K. The discrete element method for the simulation of ball

mills. *Applied Mathematical Modelling*, Vol. 16, No. 11, pp. 598–604, 1992.

[10] Kano J., Chujo N., and F. Saito. A metod for simulating the three-dimensional motion of balls under the presence of a powder sample in a tumbling ball mill. *Advanced Powder Technology*, Vol. 8, pp. 39–51, 1997.

[11] Cleary P.W. Predicting charge motion, power draw, segregation and wear in ball mills using discrete element methods. *Minerals Engineering*, Vol. 11, pp. 1061–1080, 1998.

[12] Kano J., Mio H., Saito F., and Miyazaki M. Correlation of grinding rate of gibbsite with impact energy in tumbling mill with mono-size balls. *Minerals Engineering*, Vol. 14, pp. 1213–1223, 2001.

[13] Mio H., Kano J., Saito F., and Kaneko K. Effects of rotational direction and rotation-to-revolution speed ratio in planetary ball milling. *Materials Science and Engineering*, Vol. A332, pp. 75–80, 2002.

[14] Yow H. N., Pitt M. J., and Salman A. D. Drag correlations for particles of regular shape. *Advanced Powder Technology*, Vol. 16, pp. 363–372, 2005.

[15] Kou S. *Transport Phenomena and Materials Processing*, p. 63. J.Wiley, New York, 1996.